Three component spin echo generation by radiation damping

M. P. Augustine and E. L. Hahn

Citation: The Journal of Chemical Physics **107**, 3324 (1997); doi: 10.1063/1.474683
View online: http://dx.doi.org/10.1063/1.474683
View Table of Contents: http://scitation.aip.org/content/aip/journal/jcp/107/8?ver=pdfcov
Published by the AIP Publishing

LETTERS TO THE EDITOR

The Letters to the Editor section is divided into four categories entitled Communications, Notes, Comments, and Errata. Communications are limited to three and one half journal pages, and Notes, Comments, and Errata are limited to one and three-fourths journal pages as described in the Announcement in the 1 July 1997 issue.

COMMUNICATIONS

Three component spin echo generation by radiation damping

M. P. Augustine
Department of Chemistry, University of California, Berkeley, California 94720

E. L. Hahn[a)]
Department of Physics, University of California, Berkeley, California 94720

(Received 2 June 1997; accepted 13 June 1997)

Exploration of the theory for spin–cavity coupling in inhomogeneously broadened spin ensembles shows that all three components of magnetization can be refocused. The conventional spin echo generated by two components of magnetization is a special case of this three component refocusing in the limit of negligible radiation damping. We demonstrate this effect by an analytical theorem, numerical simulation, and experiment. © *1997 American Institute of Physics.* [S0021-9606(97)05431-7]

The conventional spin echo in liquids displays partial or complete two component refocusing of x-y magnetizations that precess in a plane perpendicular to the direction of an inhomogeneous magnetic field.[1] Only in the single special case of a system being driven by a 2π hyperbolic secant pulse is it known that all three components of magnetization $M_{x,y,z}$ (u, v, and M_z in the rotating frame) vary in such a way that they return to their initial state.[2] We show by a theorem, computer simulation, and experiment that all three components can refocus completely because of the combined torque produced by a static inhomogeneous magnetic field and a spontaneously generated radiation damping reaction field. Due to the coupling between the tuned inductance and the coherent precessing spins, this reaction field causes the magnetization to emit power into the circuit resistance and align toward the ground state. Here, the precessing u and v components provide a free induction signal while M_z is altered in magnitude.

Radiation damping in nuclear magnetic resonance (NMR) has been introduced earlier[3] and discussed in a number of reviews.[4,5] In some instances the damping can distort[6] measurements of high-resolution NMR, and it is usually considered a nuisance to be eliminated or avoided.[7] In this communication we suggest that the effect may provide a useful means for NMR measurements. We treat one example of a two-pulse sequence which results in complete spontaneous three component refocusing. Although the reported effect applies to high-resolution NMR, it refers to any case that exhibits inhomogeneous line broadening and coupling to cavities in optical and microwave pumped two level systems.[8,9]

The reader is referred to the literature[10,11] regarding certain details omitted here, and only the relationships which lead directly to the development of the three component echo are presented. Conservation of energy applied to an LC circuit and the magnetization in the absence of all relaxation and demagnetization effects provides the equation

$$\ddot{\theta}+\frac{\omega}{2Q}\dot{\theta}=-\frac{\pi\gamma\omega\xi}{M_0}\int_{-\infty}^{\infty}v(\delta,t)g(\delta)d\delta. \tag{1}$$

It will be shown that this equation expresses the spontaneous radiation damping field H_1 in terms of the time-dependent angle θ that the magnetization component at exact resonance ($\delta=0$) makes with respect to the $+z$ axis. Here $\dot{\theta}=\gamma H_1$, M_0 is the total magnetization, Q is the circuit figure of merit, ξ is the rf-coil filling factor, ω is the Larmor frequency, and γ is the gyromagnetic ratio. In Eq. (1) the inhomogeneous field offset frequency is given by δ where $g(\delta)$ is defined as a normalized Lorentzian inhomogeneous field distribution function, and $v(\delta,t)$ is the absorbtive component of magnetization defined in the frame of reference rotating at frequency ω. In the usual low Q limit[5] the $\ddot{\theta}$ term can be omitted, and integration of Eq. (1) over both t' and field inhomogeneity δ yields the change in angle to be

$$\int_0^{t\to\infty}\dot{\theta}dt'=\Delta\theta=-\frac{1}{M_0T_R}\int_0^{t\to\infty}\int_{-\infty}^{\infty}v(\delta,t')g(\delta)d\delta dt', \tag{2}$$

where $\Delta\theta=\theta_f-\theta_0$. The initial angle that the magnetization makes with respect to the $+z$ axis is given by θ_0, and the radiation damping time constant T_R shown in Eq. (2) is defined in the usual way[5] by

$$T_R=(2\pi M_0\gamma Q\xi)^{-1}. \tag{3}$$

A manipulation used to explain the phenomenon of self-induced transparency[2] is applied here to transform Eq. (2) into a useful form. After substituting the Bloch equation $v(\delta,t)=\dot{u}(\delta,t)/\delta$ into the integrand of Eq. (2) and integrating over t one obtains

[a)]Author to whom correspondence would be addressed.

$$\Delta\theta = -\frac{1}{M_0 T_R}\int_{-\infty}^{\infty}\frac{u(\delta,t\to\infty)-u(\delta,t=0)}{\delta}g(\delta)d\delta. \quad (4)$$

After an rf pulse the initial value $u_i = u(\delta,t=0)=0$, and at $t=\infty$ the freely precessing final value u_f is given by

$$u_f = u(\delta,t=T+t'') = u(\delta,T)\cos\,\delta t'' + v(\delta,T)\sin\,\delta t''. \quad (5)$$

The time $T=\infty$ is chosen when the initial conditions for freely precessing u and v modes can be specified and H_1 has vanished. As u and v precess freely during time t'' beyond T, integration over the inhomogeneous distribution involves a delta function which selects only the final value of the central $v(\delta=0,T)$ mode that was at exact resonance ($\delta=0$) in the past after H_1 disappeared. Of course all the inhomogeneous spin vectors mutually cancel so that the integrated average of $v(\delta,t)$ given by $\langle v\rangle$ over the distribution is zero. Therefore $\Delta\theta$ represents the total angle through which the central vector $M(0,T)=\sqrt{M_z^2(0,T)+v^2(0,T)}$ is tipped toward the $+z$ axis from its original angle θ_0. The angle change

$$\Delta\theta = \gamma\int_0^{t\to\infty} H_1(t')dt', \quad (6)$$

is independent of the functional behavior of H_1 during time t'. Henceforth all angle changes $\Delta\theta$ are expressed in terms of the absolute values $\Delta\theta=-|\Delta\theta|$, and all tipping angles prepared by a pulse or by effects of radiation damping are confined between zero and π. Using these definitions, Eq. (4) can be recast as

$$|\Delta\theta| = \frac{1}{M_0 T_R}\int_{-\infty}^{\infty} g(0)v(0,T)\left.\frac{\sin\,\delta t''}{\delta t''}\right|_{\delta=0} d(\delta t'')$$

$$= \frac{T_2^*}{T_R}\sin(\theta_0 - |\Delta\theta|), \quad (7)$$

where $g(0)=T_2^*/\pi$ and $g(0)v(0,t)=(T_2^*/\pi)M_0\sin(\theta_0 - |\Delta\theta|)$. The experimental observation of the area under the free induction signal can be connected to $|\Delta\theta|$ as seen in Eq. (2). The graphical solution of Eq. (7) for $\theta_0=\pi/2$ is shown in Fig. 1(a) as an example. Here $y_1=|\Delta\theta|$ and $y_2 = c_n\sin(\theta_0-|\Delta\theta|)$ are ordinates and $|\Delta\theta|$ is the abscissa. By writing y_2 in this way it is clear that the constants c_n represent different possible choices for T_2^*/T_R. The intersection of y_1 with y_2 in Fig. 1(a) defines the abscissa values of $|\Delta\theta|$ acquired at $t=\infty$ for various ratios of T_2^*/T_R. Graphical solutions of Eq. (7) can be obtained for any value of the initial pulse orientation θ_0.

In this communication we are particularly interested in demonstrating the restitution of ground-state orientation as a consequence of the application of two π-pulses in succession, where the second π-pulse is applied when $H_1=0$ following the damping signal. The first π-pulse ($\pi\pm\epsilon$ where $\epsilon\ll 1$) must be slightly inaccurate so that in initial transverse v polarization can seed the start of the radiation damping signal. This manifests itself graphically in Fig. 1(b) by shifting the y_2 curve slightly to the left and permitting only one solution for $|\Delta\theta|$. The maser condition[8] $T_2^*/T_R \geqslant 1$ must also

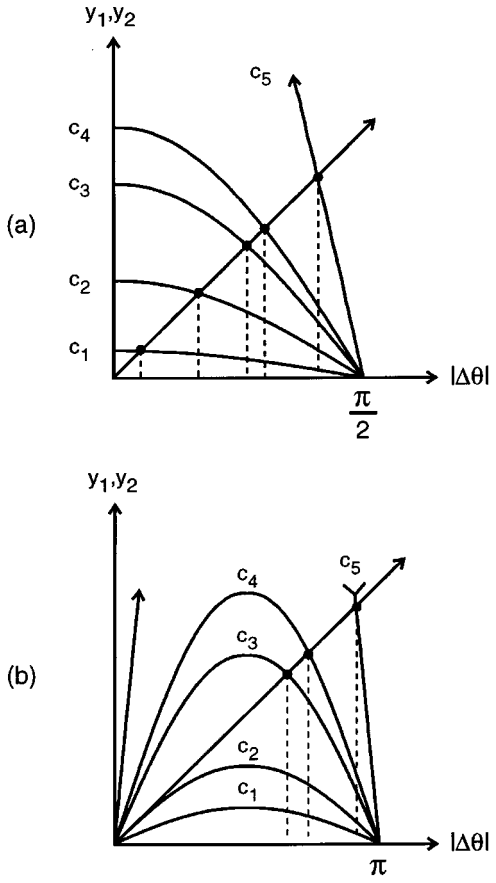

FIG. 1. Dependence of the angle changes $|\Delta\theta|$ of magnetization for different values of $c_n=T_2^*/T_R$. Here y_1 is given by $|\Delta\theta|$ and y_2 by $c_n\sin(\theta_0 - c_n\sin(\theta_0-|\Delta\theta|)$ where initial pulse tipping angles are $\theta_0=\pi/2$ in (a) and $\theta_0=\pi$ in (b). When the condition $T_2^*<T_R$ applies for an inverted system, the only solution for $|\Delta\theta|$ is zero, as shown for the c_1 curve in (b).

apply in order for the ensemble to radiate from the inverted state and tip through an appreciable angle as can be seen in Fig. 1(b) for the solutions corresponding to c_3, c_4, and c_5. A second π-pulse applied at $t''=\tau$ beyond T switches $v(\delta,T)$ to $-v(\delta,T)$ in Eq. (5). The u_f so generated becomes the initial u_i' term defined following the signal that evolves after the second π-pulse. This applies before one integrates again over the inhomogeneous distribution. The difference of the final and initial u mode distribution after the echo is again expressed, as in Eq. (5), now taking into account the altered initial conditions due to the second π-pulse. The solution for the final angle $|\Delta\theta'|$ in terms of $|\Delta\theta|$ is then given by

$$|\Delta\theta'| - |\Delta\theta| = -\frac{T_2^*}{T_R}\sin(|\Delta\theta'| - |\Delta\theta|). \quad (8)$$

For any value of T_2^*/T_R the angle change after the first π-pulse for $M(0,T)$ becomes the initial angle defined as $\theta_0' = |\Delta\theta|$ for the transformed vector labeled as $M(0,T')$. Following transformation by the second π-pulse, the angle change of $M(0,T')$ is given by $|\Delta\theta'|$. This angle is the same as the angle change $|\Delta\theta|$ that $M(0,T)$ tipped through after the first π-pulse. The net effect is that $M(0,T')$ aligns along

the $+z$ axis, and $|\Delta\theta'|-|\Delta\theta|=0$. This is the only physical solution of Eq. (8) because the final angle change is identical to that accumulated before application of the second π-pulse. Equation (8) shows that the magnetization will refocus but does not provide any information about when the echo maximum following the second π-pulse will occur. With reference to the usual two component spin echo, the maximum of the three component echo will be set by the time between the signal maximum after the first π-pulse and application of the second π-pulse, not by the pulse spacing. The effect of two pulse sequences using rotations θ_1 and θ_2 other than π will be treated at length in a later paper.

The computer simulations of the $\pi\pm\epsilon-\pi(\epsilon=0.01°)$ pulse sequence shown in Figs. 1 and 4 were generated by numerically integrating the Bloch equations with terms added to account for the effects of radiation damping.[4] In the particular case of $T_2^*/T_R=2.56$ and a Lorentzian distribution $g(\delta)$, the computational average $\langle M_z(T)\rangle=0$, and Fig. 1(b) yields $|\Delta\theta|=7\pi/10$. Figure 2(a) shows the anticipated echo formation for this special case after a second π-pulse at 200 ms. It is important to note that although the on-resonance component $M_z(0,T)$ is nonzero and $|\Delta\theta|>\pi/2$ applies, the integral over all δ allows the average $\langle M_z(T)\rangle$ to be zero. Figure 2(b) demonstrates what happens to $\langle v\rangle$ and $\langle M_z\rangle$ during this echo sequence when T_2^*/T_R is increased from 2.56 to 5.00. Here $\langle M_z\rangle$ increases to 0.5 before application of the second π-pulse at 200 ms.

The remarkable transformation of all of the inhomogeneously distributed vectors from the $-z$ to $+z$ orientation shows that the phase relations developing among them during spontaneous signal generation are quite complicated and nonlinear. Yet the precession about changing effective fields due to the combination of static field gradients and the changing radiation damping field in the rotating frame proves to be reversible as in the conventional spin echo.[1] There is a new variation—the ensemble reverts to another energy state (in our example from $-M_zH_0$ to $+M_zH_0$) because power must be transferred collectively from the spin ensemble to the tuned circuit resistance. This can only occur if the third component M_z changes with u and v in the refocusing process. One must note that the analytical theorem used here may pertain to any inhomogeneous field distribution $g(\delta)$ of defined symmetry. Any peculiar holes or bumps in the distribution may cause complicated beats and signal distortion that are best treated numerically.

Previous treatments of radiation damping effects in NMR have been restricted to the special case of a sharp line. Only in the limit of an exponentially changing magnetization can a Lorentzian inhomogeneous field distribution be taken into account by adding a $1/T_2^*$ phenomenological rate term to Bloch's equations.[12,13] Such analytical treatments are accurate for a single homogeneously broadened line but they cannot in general account for radiation damping effects determined by interference among inhomogeneous magnetization components. This point is best made by comparison with experiment as shown in Fig. 3 for a proton π-π pulse sequence applied to water at 11.74 T. Figure 3(a) shows the expected result for water in a well shimmed magnet. Radiation damping quickly restores the inverted magnetization fully to the $+z$ direction following the first pulse. Thus, the behavior of the magnetization following the second π-pulse at $t=600$ ms is identical to that after the first π-pulse. Figure 3(b) shows that a different effect occurs when the water line is homogeneously broadened from 21 to 27 Hz by adding a paramagnetic relaxation agent to the sample. The additional linewidth in this case does not allow the magnetization to fully recover along the $+z$ direction. Therefore only a small fraction of the full magnetization M_0 can contribute to T_R following the second π-pulse. The radiation damping becomes negligible and minimal signal is seen after the second π-pulse applied at 600 ms.

The usual conditions encountered in high-resolution NMR experiments present linewidths dominated by inhomo-

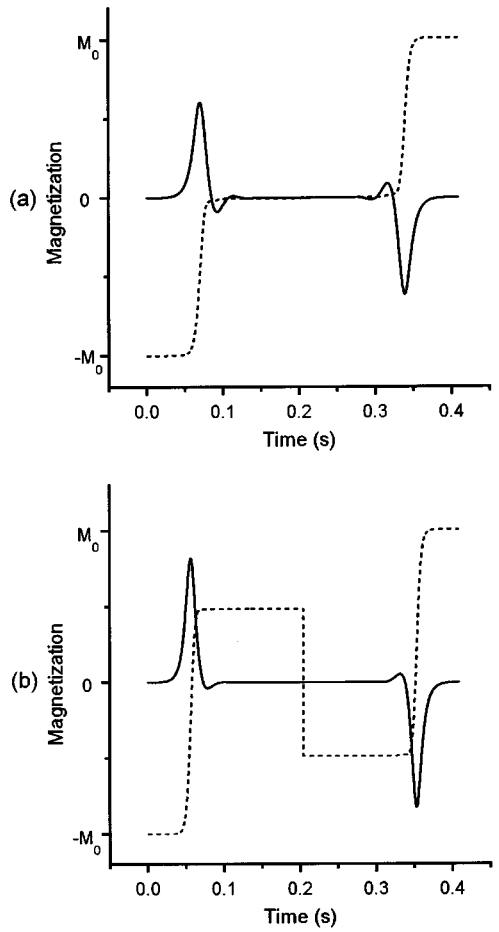

FIG. 2. Numerical simulation of three component refocusing by applying two π-pulses having the same phase and separated by 200 ms. Here $T_R=5$ ms was chosen so that the maximum of $\langle v\rangle$ (solid line) in the narrow line limit occurs at $t=50$ ms and $\langle M_z\rangle$ (dashed line) nearly recovers to full alignment along the $+z$ direction following the first π-pulse. In (a) the field homogeneity was adjusted to give $T_2^*=12.8$ ms producing $T_2^*/T_R=2.56$ and $\langle M_z\rangle=0$ at 200 ms, prior to the second π-pulse. The second π-pulse flips the transverse magnetization as discussed in the text and the echo maximum appears ~150 ms later. Increasing T_2^* to 25 ms allows $\langle M_z\rangle$ to partially recover to its equilibrium value in (b) before the second π-pulse. Again an echo maximum appears ~150 ms later. Note that in both (a) and (b) there is a low-frequency oscillation following the signal maximum after the first π-pulse and before the echo after the second π-pulse. These oscillations, revealed by computer analysis here, have been observed experimentally in the literature following one π-pulse and warrant further study.

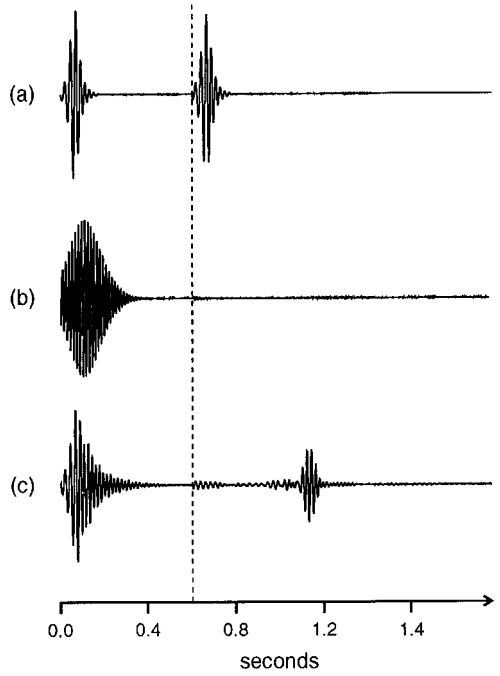

FIG. 3. Experimental verification of three component refocusing for protons in a 90% $H_2O-10\%D_2O$ solution observed at 11.74 T using a General Electric Omega NMR spectrometer. The free induction decays shown here correspond to an offset frequency of 50 Hz for a well shimmed water line having a full width at half maximum of 21 Hz. In (a) the maximum of the signal following the second π-pulse applied at 600 ms is consistent with the magnetization having nearly reoriented completely along the $+z$ direction after the first π-pulse. This corresponds to $T_2^*/T_R \gg 1$ as shown in Fig. 1(b) for $T_2^*/T_R > c_5$ so that $|\Delta\theta| \sim \pi$. In (b) the homogeneous linewidth of the sample is increased to a broadening of ~27 Hz by adding a small amount of paramagnetic manganese (II) chloride (0.1 mM). This increases the time at which the radiation damping signal appears from 50 ms in (a) to 100 ms in (b) and eliminates the radiation damping signal following the second pulse. Increasing the inhomogeneous linewidth of the original water sample to 29 Hz by adjusting the magnetic-field shims produces the anticipated three component refocusing at ~1.15 s, as shown in (c).

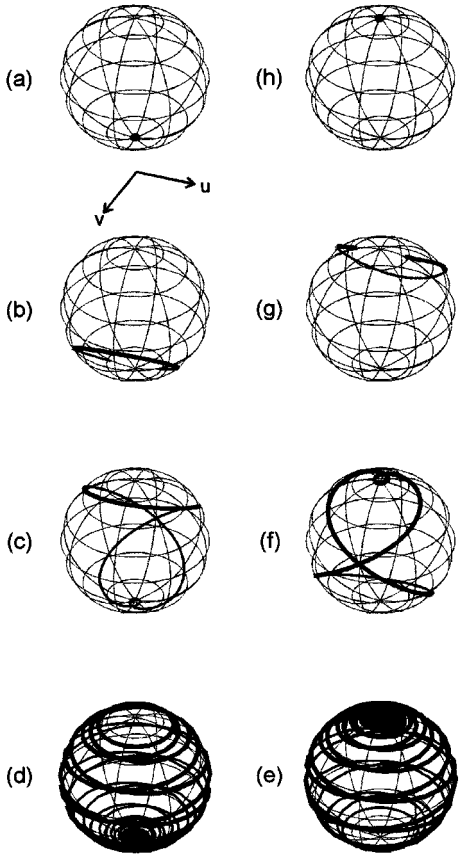

FIG. 4. Spatial distribution of the endpoints of isochromats projected onto a unit sphere (solid black line) at given times from (a)–(h) for the π-π pulse sequence for $T_2^*/T_R = 5.00$. The sequence and parameters apply to those of Fig. 2(b). The integral of the x, y, and z components of these isochromats weighted by $g(\delta)$ indicate $\langle v \rangle$, $\langle u \rangle$, and $\langle M_z \rangle$ respectively. Immediately following the first $\pi \pm \epsilon$ ($\epsilon = 0.01°$) pulse all of the isochromats are aligned along the $-z$ direction as shown by the dot at the south pole in (a). As time proceeds, an observable signal develops and the magnetization vectors spread out in a circular pattern in three dimensions on the unit sphere. The diameter of this circle continues to increase to a maximum, as shown in (b) at a time $t = 57$ ms [Fig. 2(b)] corresponding to the maximum of the damping signal. As each isochromat tends to precess about the changing effective field direction, the circular pattern evolves into a figure eight and then into two connected orbitals seen in (c) for $t = 75$ ms. Finally, when H_1 vanishes, an extremely complex array of connected orbits spreads over the surface of the unit sphere, averaging the magnetization to produce zero signal and resulting in a small value for $\langle M_z \rangle$. This state of free precession at $t = 200$ ms is shown in (d). The effect of the second π-pulse at 200 ms is to invert (d) to the (e) configuration. The isochromats then exhibit a reversal of phase accumulated in the (a)–(d) sequence. This is seen in (f) at $t = 325$ ms and (g) at the echo maximum occurring at $t = 343$ ms. Finally the magnetization refocuses along the $+z$ direction at $t = 400$ ms after H_1 has vanished.

geneous broadening. The results of the π-π pulse sequence on the same water sample used for Fig. 3(a) are shown in Fig. 3(c). Here additional linewidth is introduced by partially deshimming the magnet to provide a 29 Hz inhomogeneously broadened water line of nearly the same width at the 27 Hz homogeneously broadened line in Fig. 3(b). The maximum amplitude of the signal following the second π-pulse does not occur at 50 ms as in Fig. 3(a) after the first π-pulse, but at a time proportional to the pulse spacing of 600 ms. We attribute this signal to a spontaneously generated three component spin echo. The decreased echo amplitude in comparison to the signal following the first π-pulse results from T_1 and T_2 relaxation and diffusion on the time scale of the experiment, 2 s, while the low amplitude signals flanking the echo in Fig. 3(c) reflect an asymmetric inhomogeneous spectrum produced by deshimming the magnet.

The complex spontaneous reversal and reorientation of the nuclear magnetization components during radiation damping for the π-π pulse sequence with $T_2^*/T_R = 5.00$ is shown in Fig. 4. The distribution of the isochromat endpoints on a unit sphere is seen to be scrambled into an ostensible chaotic array in three dimensions. Nevertheless, the π-π pulse sequence allows a complete refocusing of all the components of magnetization into complete alignment along the $+z$ axis. The Lorentzian weighted average of these isochromats is shown in Fig. 2(b).

Can this property of refocusing be of any use? By taking into account the unusual property of three component free induction signals, one may conceive of pulse sequence and field gradient manipulations very much like those that have been developed for pulsed NMR. Consider a double resonance experiment in which an abundant spin species under-

goes three component refocusing. This damping signal can serve as a detector of a second spin species coupled by either the nuclear Overhauser effect or a scalar coupling. Even if only a fraction of the inhomogeneous spectrum of the abundant spins is coupled to the second spin, the perturbation of that fraction should be amplified by the radiation damping signal because of coupling through the tuned circuit to all parts of the inhomogeneous line. Other properties of the three component refocusing effect are strangely different from the ordinary two component case. For example, the ordinary stimulated echo following a three pulse sequence (e.g., the $\pi/2$-$\pi/2$-$\pi/2$ sequence) is independent of the defocusing and refocusing of u and v components prior to the third pulse because M_z remains constant. In the three component case, however, M_z is also changing with u and v during this time. We find, for example, that the radiation damped stimulated echo from a π-$\pi/2$-$\pi/2$ sequence is small compared to a maximum stimulated echo following a π-$\pi/2$-π sequence. A discussion of the new properties that result from three component refocusing will be treated in detail in a future publication.

The authors are indebted to Alex Pines for fruitful discussions, Jeff Reimer for a careful reading of this manuscript, and Ho Cho for guidance in the course of data acquisition. E.L.H. thanks Alex Pines for support during the course of this work and M.P.A. gratefully acknowledges the National Science Foundation Postdoctoral Fellowship program under Grant No. CHE-9504655. This work was supported by the Director, Office of Energy Research, Office of Basic Energy Sciences, Materials Sciences Division of the U.S. Department of Energy under Contract No. DE-AC03-76SF00098.

[1] E. L. Hahn, Phys. Rev. **80**, 580 (1950).
[2] S. L. McCall and E. L. Hahn, Phys. Rev. **183**, 457 (1969).
[3] N. Bloembergen and R. V. Pound, Phys. Rev. **95**, 8 (1954).
[4] S. Bloom, J. Appl. Phys. **28**, 800 (1957).
[5] W. S. Warren, S. L. Hammes, and J. L. Bates, J. Chem. Phys. **91**, 5895 (1989).
[6] P. R. Blake and M. F. Summers, J. Magn. Reson. **86**, 622 (1990).
[7] P. Broekaert and J. Jeener, J. Chem. Phys. **103**, 5886 (1995).
[8] P. Bosiger, E. Brun, and D. Meier, Phys. Rev. Lett. **38**, 602 (1977).
[9] M. S. Feld and J. C. MacGillivary, *Coherent Nonlinear Optics*, edited by M. S. Feld and V. S. Letokhov (Springer-Verlag, Berlin, 1980).
[10] E. L. Hahn, *NMR and More—A Festschrift in Honor of Anatole Abragam*, edited by M. Goldman and M. Porneuf (Les Editions de Physique, France, 1994), p. 235.
[11] E. L. Hahn, Concepts Magn. Reson. **9**, 65 (1997).
[12] X. A. Mao and C. H. Ye, Concepts Magn. Reson. **9**, 173 (1997).
[13] T. M. Barbara, J. Magn. Reson. **98**, 608 (1992).